

Optimization of honeycomb battery package based on space mapping algorithm

Wenquan Shuai¹, Xin Luo¹, Hu Wang^{*1,2},

¹State Key Laboratory of Advanced Design and Manufacturing for Vehicle Body, Hunan University, Changsha, China

²Joint Center for Intelligent New Energy Vehicle, Shanghai, China

Jian Wang³

ABSTRACT

A new honeycomb battery package structure is designed in this study. It's a honeycomb structure but using a grid to reinforce its strength. It can not only satisfy the requirements of strength but also reduce the mass of battery package. To obtain the highly accurate finite element (FE) model, the material parameters of 18650 cylindrical Li-ion battery are identified by using optimization techniques based on flat compression test data. Due to the expensive cost of finite element evaluation, the space mapping (SM) algorithm is suggested to optimize the structure of the package. Compared with other space mapping algorithms, the coarse model of space mapping is based on a pseudo-plane-strain model. Moreover, to guarantee the reliability, the mean and variance values of battery stress are used to be the objective function. The final optimum shows that the maximum stress of inner battery is decreased from 32.1733MPa to 12.9642MPa, the mean of battery stress is decreased from 5.3231MPa to

*Email: wanghu@hnu.edu.cn, Tel 86-731-88821417, Fax 86-731-88821807

3.5836MPa and the variance is decreased from 5.9944 to 4.3904. It means the magnitude of stress and the distribution of stress are improved significantly.

Keyword: Li-ion battery package; Optimization; Simulation; Space mapping(SM) algorithm

1. Introduction

The Li-ion battery is considered to be an ideal electric vehicle battery due to its higher energy density, higher power density and longer cycle life. However, the safety of the cell should be more valued. When the cell is abused, it might explode or get fire due to internal short circuit [2]. These abuses include mechanical abuse, overcharge, over-discharge and overheating. In this work, only mechanical abuse is concerned. In order to understand the mechanism of internal short circuit, experiments are conducted. However, these experiments are ruinous and unrepeatable. Therefore, FE method is commonly used to simulate and predict the behavior of battery. However, it is difficult to develop the constitutive model of Li-ion battery when build the FE models. Several researchers have completed a lot of works for this problem. Sahraei *et al.*, (2012a) performed mechanical test on pouch battery under five loading conditions and used compressible foam to build FE models of pouch battery. Wierzbicki and Sahraei (2013) constructed FE models of 18650 Li-ion battery and studied the homogenized mechanical properties of the battery. Greve and Fehrenbach (2012) performed quasi-static mechanical test on cylindrical battery and built a macro-mechanical FE model to simulate the deformation and short circuit initiation of cylindrical battery. Sahraei *et al.*, (2012b) modeled 18650Li-ion battery and

obtained the short circuit detection criterion under mechanical abuse condition. Ali *et al.*, (2013) used computational models of Li-ion battery to simulate the behavior of battery under constrained compression tests. Sahraei *et al.*, (2014) tested three types of pouch battery ranging from small cells to large cells under several global and local compression conditions. They also constructed models for these three types of battery and investigated conditions leading to internal short circuit in the cells. Sahraei *et al.*, (2016) developed a micro model of representative volume element (RVE) in Li-ion battery to study failure mechanisms of internal component under complex loading scenarios. The available model for applying can be created based on these achievements.

In this study, the new battery pack structure is suggested. Compared with the typical honeycomb structure, the distinctive characteristic of this structure is that it uses a grid to reinforce the strength [1]. It is well known that typical honeycomb structure is an excellent function structure which has outstanding crashworthiness and energy-absorption property. Therefore it has been widely used and investigated. Yamashita and Gotoh (2005) utilized numerical simulation to analyze effect of honeycomb cell shape and foil thickness on crush strength of honeycomb which is compressed in the longitudinal direction. Ivañez *et al.*, (2017) studied the influence of structure size and material properties for energy-absorption property of honeycomb core. Zhang *et al.*, (2017) investigated the indentation response and energy absorption of honeycomb sandwich panels under drop-weight impact behavior and obtained some semi-empirical formulations under different impact energy. However, the typical honeycomb structure is too soft to be used as battery package structure directly. It should be

reinforced its strength by grid, and the largest difference from typical honeycomb is that the honeycomb is not applied as buffer structure of battery package. The batteries are placed into its hexagon cells, so that the special hexagon cell is utilized to protect internal battery.

In order to obtain better performance of battery package structure, optimization should be conducted. However, the computational cost of FE model is too high. It results in that typical direct optimization algorithm cannot be used in this problem. Space mapping (SM) algorithm is an efficient optimization method, especially for complex problems. The SM algorithm would establish two types of model that are fine model and coarse model, respectively. Fine model is a high accurate model or evaluation, it requires high computational cost but achieves a more accurate result. Coarse model is much simpler and achieves a result efficiently, but the accuracy of the result is lower. The SM would establish a mapping relation between response of fine model and coarse model. The method can get the optimized result of coarse model in a short time, and then obtain the optimized result of fine model through the mapping relation. Leary *et al.*, (2001) used constraint mapping method to optimize an expensive model. The method mapped the coarse model constraints so that the coarse model constraints can approximate the fine model constraints. It is accurate to apply in an expensive model whose real objective varies little but constraints changes signally. Redhe *et al.*, (2013) used the SM algorithm which uses surrogate models and response surface method (RSM) to optimize a series of vehicle crashworthiness problems. Florentie *et al.*, (2016) applied the SM algorithm in fluid-structure interaction problems. The output SM was used to optimize partitioned fluid-structure

interaction problems, and resulting in the computational cost decreased to 50% in comparison with quasi-Newton method. Wang *et al.*, (2016) integrated reanalysis method with SM method to propose an available optimization method. The Reanalysis-based space mapping method showed a significant improvement in the efficiency of expensive simulation-based problems. Due to above mentioned advantages, the SM algorithm seems to be suitable for the problems with highly computational cost. Therefore, the SM is applied to structure optimization of honeycomb package in this study.

The rest of paper is organized as follows. In section 2, the material parameters of Li-ion battery are obtained by the inverse identification. What's more, the material parameters of Al alloy are obtained from uniaxial tensile test. In section 3, the modeling method of battery package is validated by experiments and then the fine FE model of battery package is established and an available coarse FE model is proposed. In section 4, trust region SM (TRSM) algorithm is introduced and used to optimize the battery package structure. In the final section, the conclusions are made.

2. Identification of material parameters of Li-ion battery and Al alloy 6061-T6

2.1 Inverse identification of material parameters of battery

2.1.1 Inverse identification method

For the battery package design, it is important to use high accurate FE evaluation in the optimization procedure. The material parameters is the critical issue to the

accuracy of simulation. To guarantee the accuracy of the FE evaluation, the hybrid numerical method is used to obtain the material parameters in this study. The flow chart of the inverse identification method is shown in Fig. 1.

2.1.2 Flat compression test of 18650 battery

The Li-ion batteries that were studied in this work are commercial 18650 ternary polymer lithium batteries. Their capacity is smaller than pouch battery's, is only 2600mAh. It means an electric vehicle needs more batteries than using pouch battery. However, they are safer than pouch battery. The specifications of these 18650 batteries are detailed in Table 1.

The contribution of shell casing to total force was less than 1% in the flat compression test [5]. Therefore, whether there is or not shell casing is not important for the test. In order to measure the voltage of battery, the shell casing is retained, as shown in Fig. 2(a). The compression test was conducted in INSTRON 150kN Universal Test Machine, and digital image correlation (DIC) was used to measure local strain (Fig. 2(c)). The UNI-T U322 Thermometer and UNI-T UT61C Multimeter were used to obtain temperature and voltage respectively.

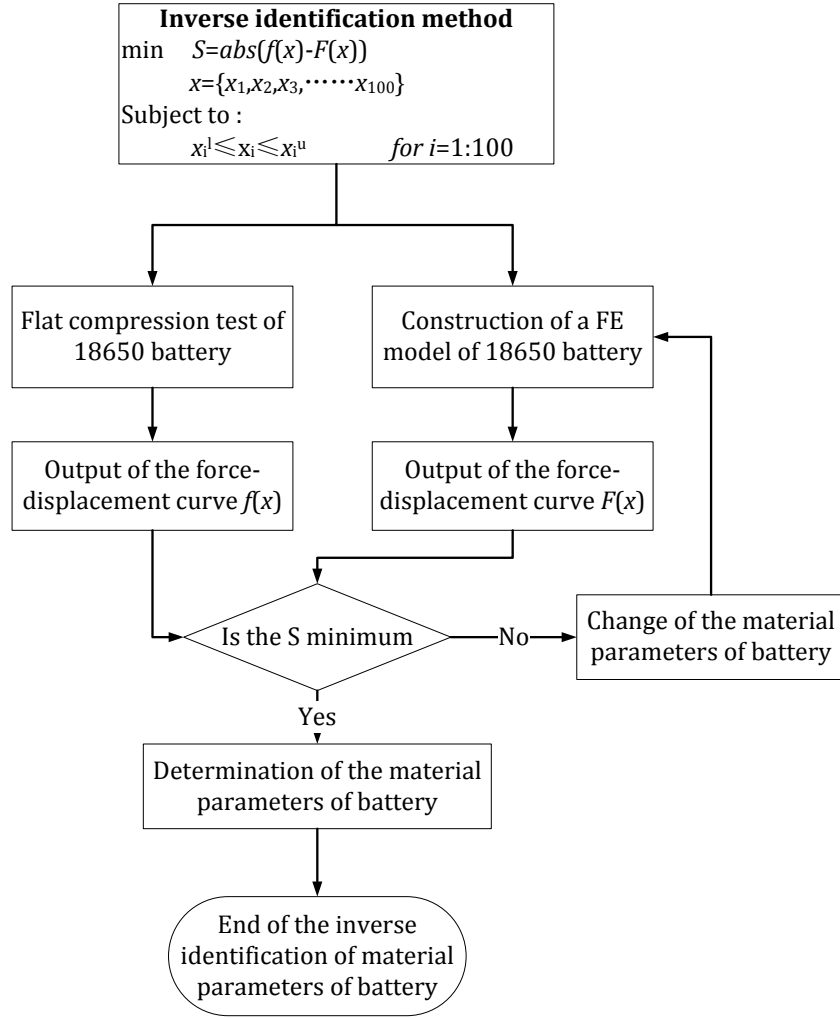


Fig. 1 The flow chart of the inverse identification method

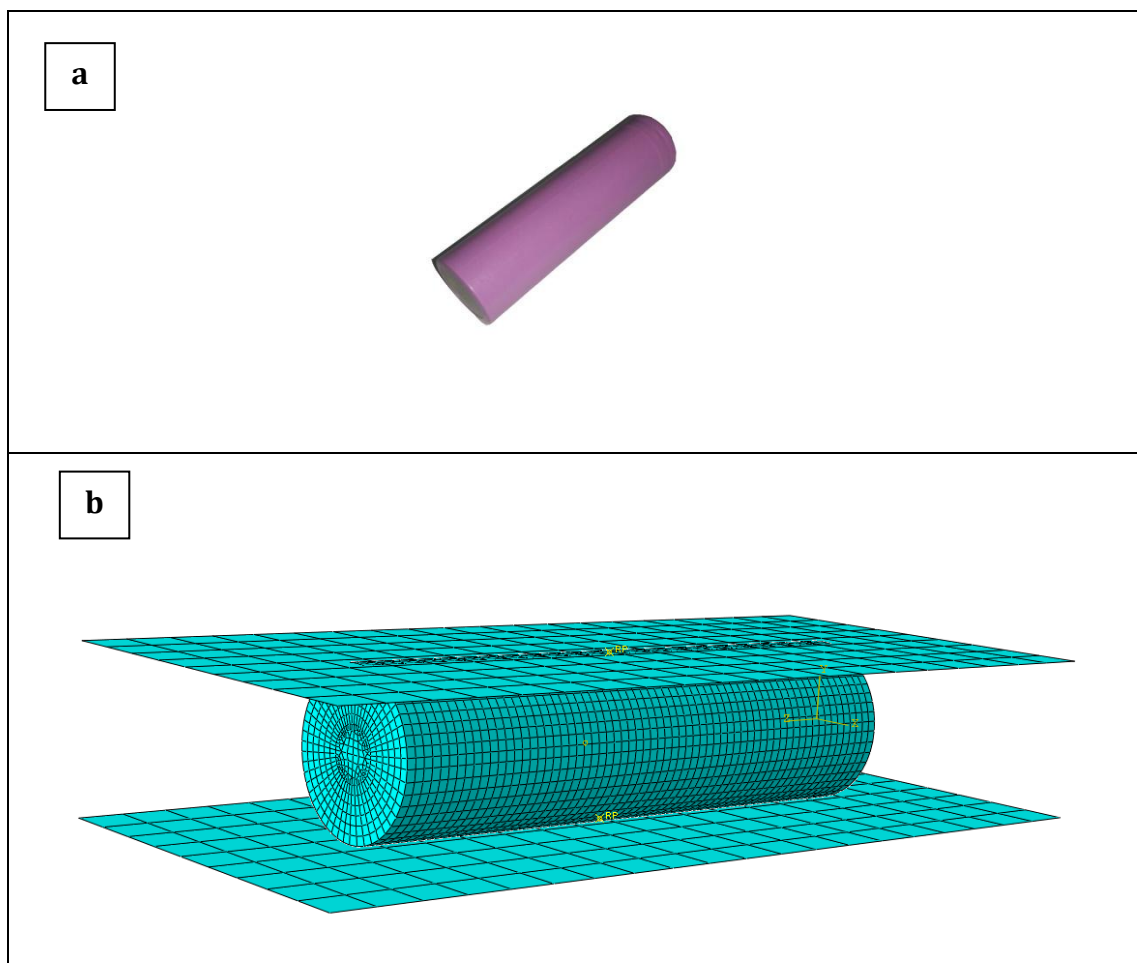
When test was started, the deformation rate was set as 1mm/min. When the internal short circuit happens, the test would be stopped. The response of internal short circuit is that the load and the voltage dropped rapidly and the temperature increase simultaneously [2].

The force, displacement, temperature and voltage were measured in the test. After the test, the electrolyte of battery was all leaked and the shell casing was flawed. The battery after deformation is shown in Fig. 2(d). Figure. 2(e) shows

the result data which obtained in the test. The data reveals the load dropped rapidly from $5.7 \times 10^4 \text{N}$ when the displacement was about 6.3mm. Meantime, the temperature started increase significantly and the voltage dropped from 3.6V to 0.096V in a short time. These phenomena mean that internal short circuit has happened.

Table 1
Specifications of the 18650 battery

Parameters	Values
Nominal capacity	2600mAh
Size	18mm*18mm*65mm
Weight	48g
Nominal voltage	3.7V
material	$\text{Li}(\text{NiCoMn})\text{O}_2$
Operating temperature	$-20^\circ\text{C} - 60^\circ\text{C}$



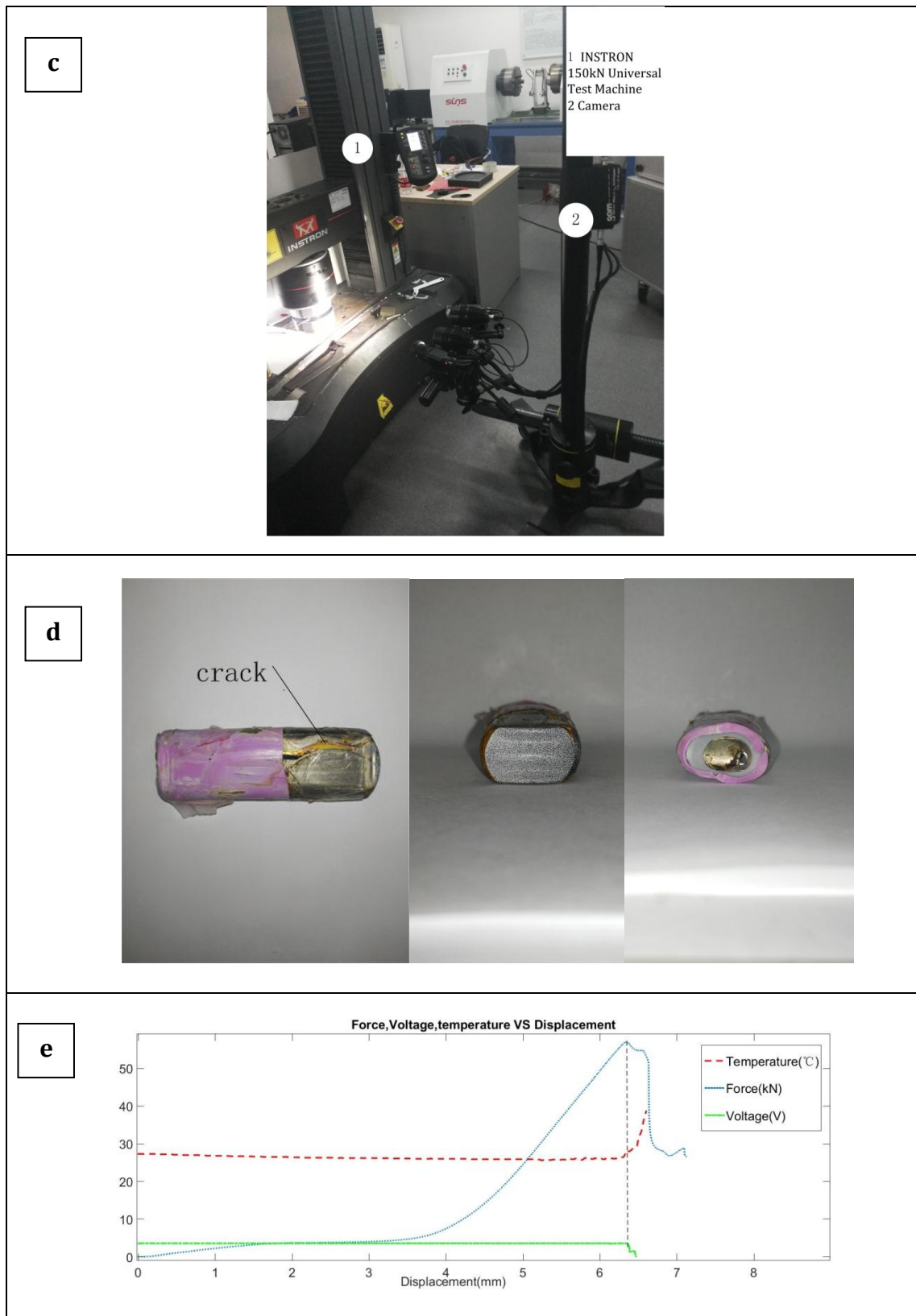


Fig. 2 (a) The entity of battery (b) The FE model of battery (c) The experimental facilities of the flat compression test (d) The deformed battery (e) The result of the flat compression test

2.1.3 FE model of 18650 battery

A FE model of 18650 battery was constructed in ABAQUS. The whole cell is regarded as a homogeneous and isotropous material. The crushable foam is used as the constitutive model of the material[3]. To simulate the real compression test, the model of the cell is compressed by two rigid shells. The cell is modeled by using 8-node linear brick and reduced integration solid elements (C3D8R). The simulation parameters are detailed in Table 2. The whole model is shown in Fig. 2(b). The contact force between rigid board and battery is exported as history output.

Table 2

The simulation parameters of battery FE analysis

Parameters	Values
Global seed size of the cell	1mm
Global seed size of the rigid shell	5mm
Simulation step	Dynamic explicit; 0.12s
Loading speed	50mm/s
Friction coefficient	0.1

2.1.4 Inverse identification of material parameters of battery

The material parameters of the cell are obtained by inverse identification method. The inverse identification method is an optimization method essentially. Two force-displacement curves could be obtained by experiments and simulation, respectively. The target is minimizing the error between two force-displacement curves. There are 11 design variables in this inverse identification problem. Each FE evaluation output 200 sets of data of contact force and time, and the interval between two sources is about 0.0006s or 0.03mm. Similarly, the experiment output 4312 sets of data of force and displacement. The interval between two sources is about 0.002mm. The 100 sets of simulation data are

selected to calculate the error. The selection rule is that the data with even index are selected. $f(x_1)$ represents the contact force when the displacement is x_1 in simulation. $F(x_2)$ represents the force when the displacement is x_2 in experiments. The objective function is

$$\begin{cases} \min_D \sum_{i=1, j}^{100} (f(x_i) - F(x_j))^2 \\ D = [E \ \nu \ \sigma_1 \ \sigma_2 \ \sigma_3 \ \sigma_4 \ \sigma_5 \ \sigma_6 \ \sigma_7 \ \sigma_8 \ \sigma_9] \end{cases} \quad (1)$$

where x_j is the nearest displacement from the x_i in the experimental displacement data. D represents the design variables where E is elasticity modulus, ν is Poisson ratio, $\sigma_{1 \rightarrow 9}$ is yield stress in harden curve which shown in Table 3. The Genetic algorithm (GA) algorithm is used to obtain the inverse identification result.

The inverse identification result is shown in Table 4. Figure. 3(a) shows the force-displacement curves of experiments and simulation. Figure. 3(b) shows the stress contours of battery. The R-square of the two curves is 0.9. Therefore, the inverse identification parameters can be accepted.

Table 3

The harden curve of material of battery

Yield stress/MPa	Plastic strain
$\sigma_0=7.6958$	0
σ_1	0.010
σ_2	0.025
σ_3	0.065
σ_4	0.100
σ_5	0.125
σ_6	0.165
σ_7	0.215
σ_8	0.255
σ_9	0.325

Table 4

The material parameters of battery

Parameters	Values	Unit
E	544.8866	MPa
ν	0.0234	
σ_1	9.4787	MPa
σ_2	7.7454	MPa
σ_3	7.8069	MPa
σ_4	7.7137	MPa
σ_5	7.6989	MPa
σ_6	7.7091	MPa
σ_7	10.1857	MPa
σ_8	106.6688	MPa
σ_9	161.4426	MPa

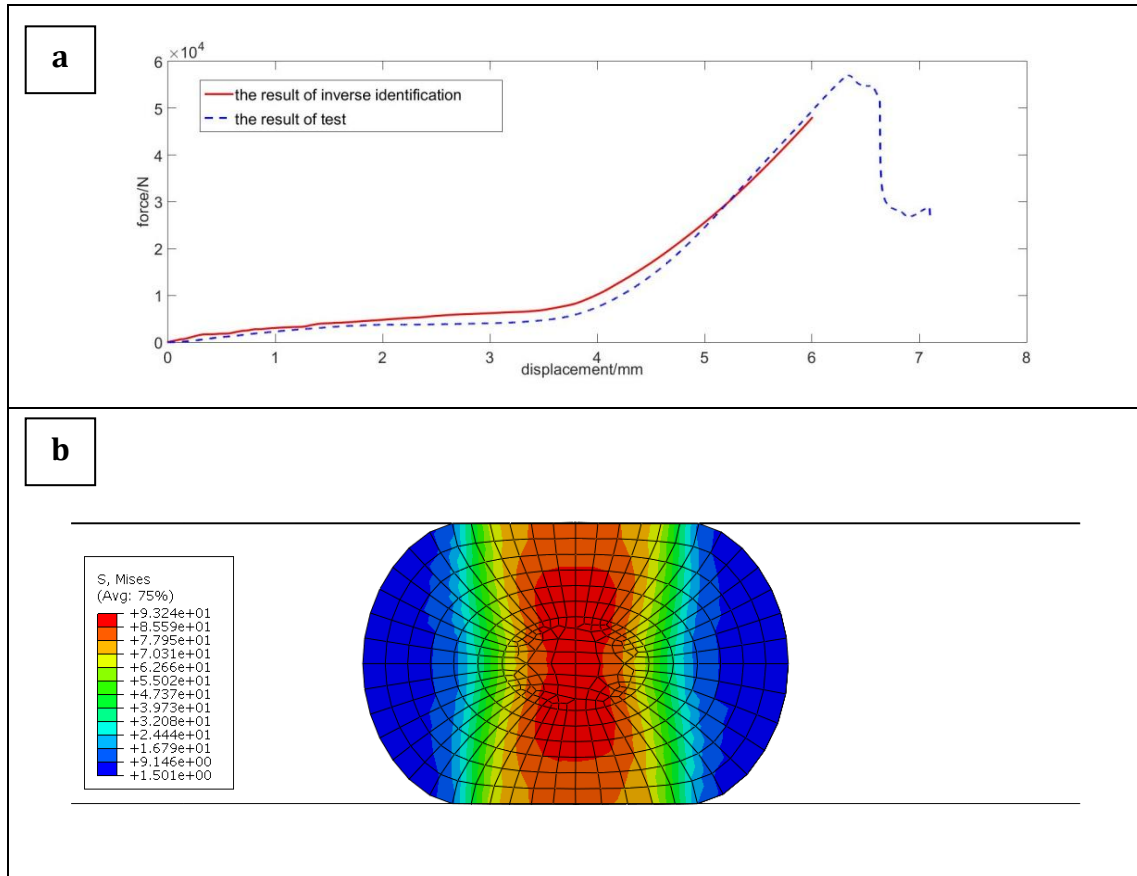
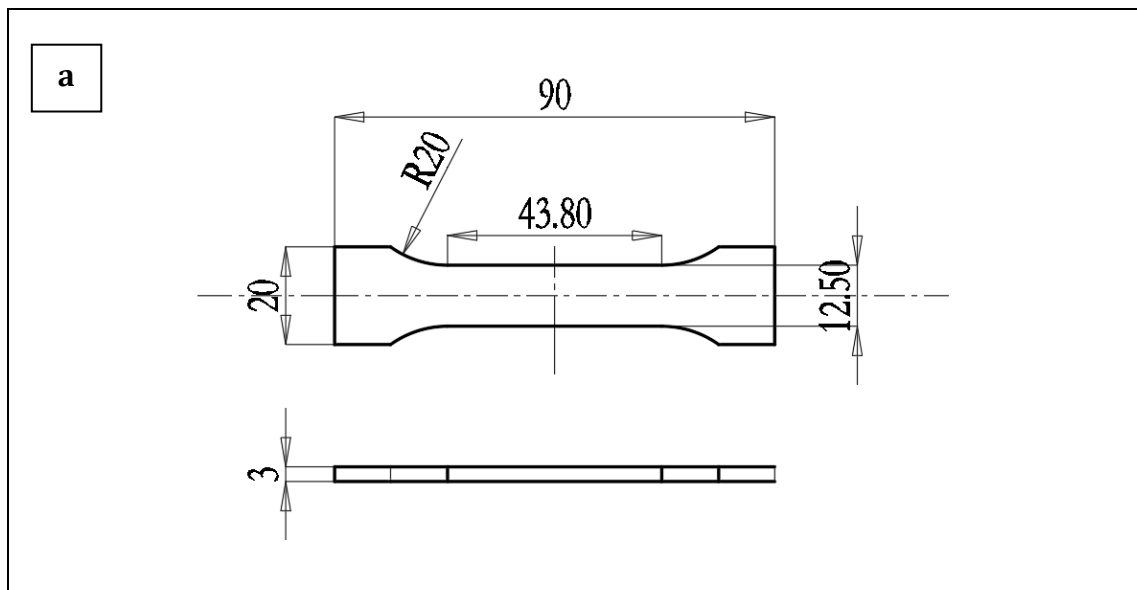


Fig. 3 (a) The force-displacement curves of experiments and simulation (b) The stress contours of battery

2.2 The material parameters of Al alloy 6061-T6

2.2.1 Uniaxial tensile test of Al alloy 6061-T6

The material of the battery package is Al alloy 6061-T6. In order to obtain the material parameters of Al alloy 6061-T6, the uniaxial tensile test was conducted. The size of tensile test coupon is obtained according to GB/T 228-2010, it is shown in Fig. 4(a). The uniaxial tensile test was conducted in INSTRON 150kN Universal Test Machine. To obtain the strain of tensile test coupon during the test, the extensometer was used. The tensile rate was 2mm/min. Figure. 4(b) shows the fractured tensile test coupon. The strain-stress curve obtained from test is shown in Fig. 4(c).



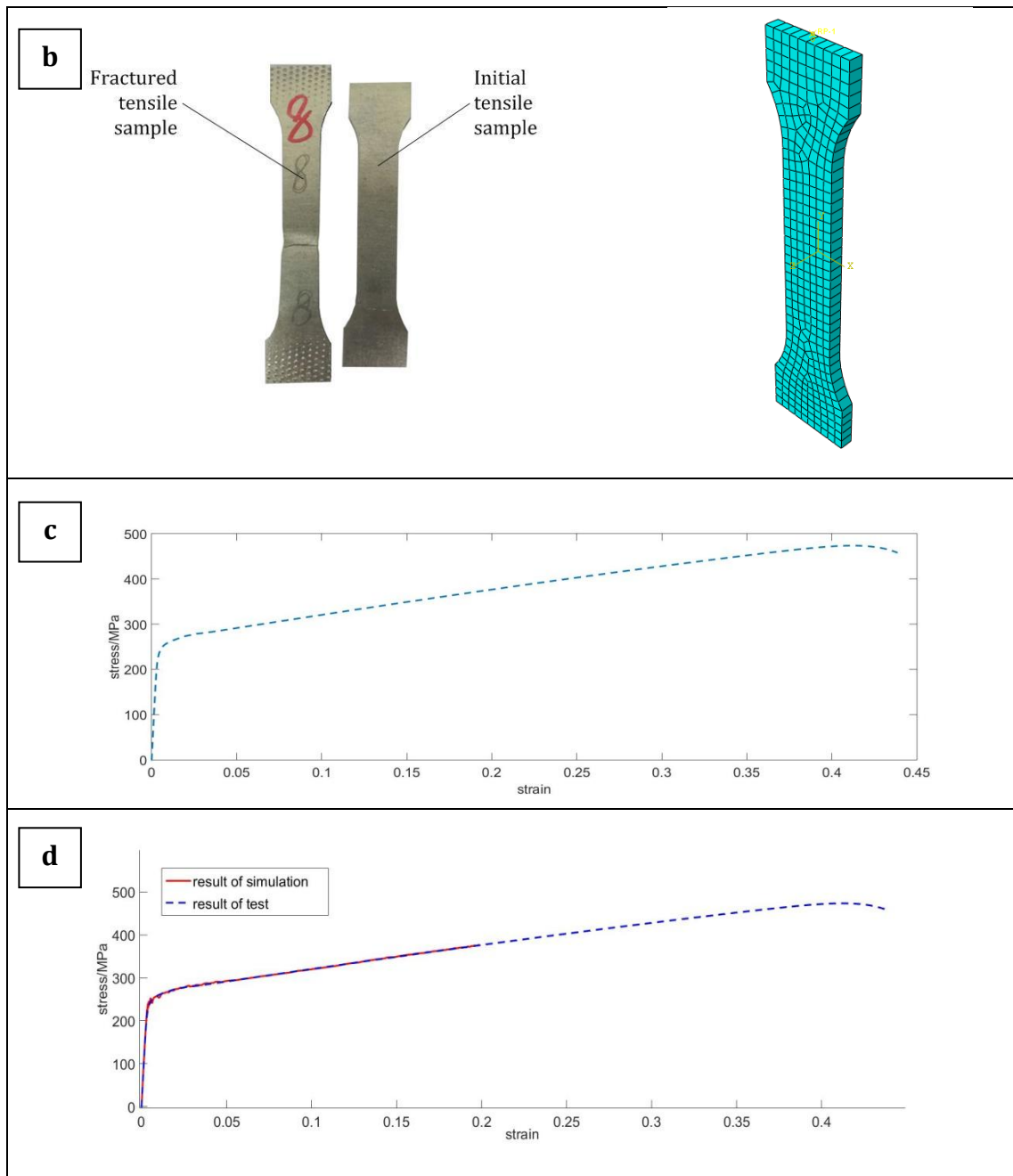


Fig. 4 (a) The size of tensile test coupon (b) The fractured tensile test coupon and corresponding FE model (c) The strain-stress curve of tensile test (d) The result curves of parameters validation

2.2.2 Validation of material parameters of Al alloy 6061-T6

According to the above illustration, the material parameters can be obtained from the strain-stress curve. The material parameters of Al alloy 6061-T6 are

summarized in Table 5. In order to validate the material parameters, the FE model of tensile sample has been built, as shown in Fig. 4(b). The strain-stress curve of elements of FE model is output to validate the accuracy of parameters. The validation result is shown in Fig. 4(d). The result indicates the material parameters of Al alloy are accurate.

Table 5

The material parameters of Al alloy

Elasticity modulus /MPa	71.275	
Poisson ratio	0.33	
Yield strength/ MPa	241.5	
Density/ (T/mm³)	2.9e ⁻⁹	
Plastic curve	Yield stress/MPa	Plastic strain
	241.5	0
	263.0	0.0069
	278.8	0.0217
	318.8	0.0921
	346.7	0.1408
	374.5	0.1914
	388.8	0.2181
	423.8	0.2862
	464.3	0.3728
	473.6	0.4078

3. Fine and coarse FE models of battery package

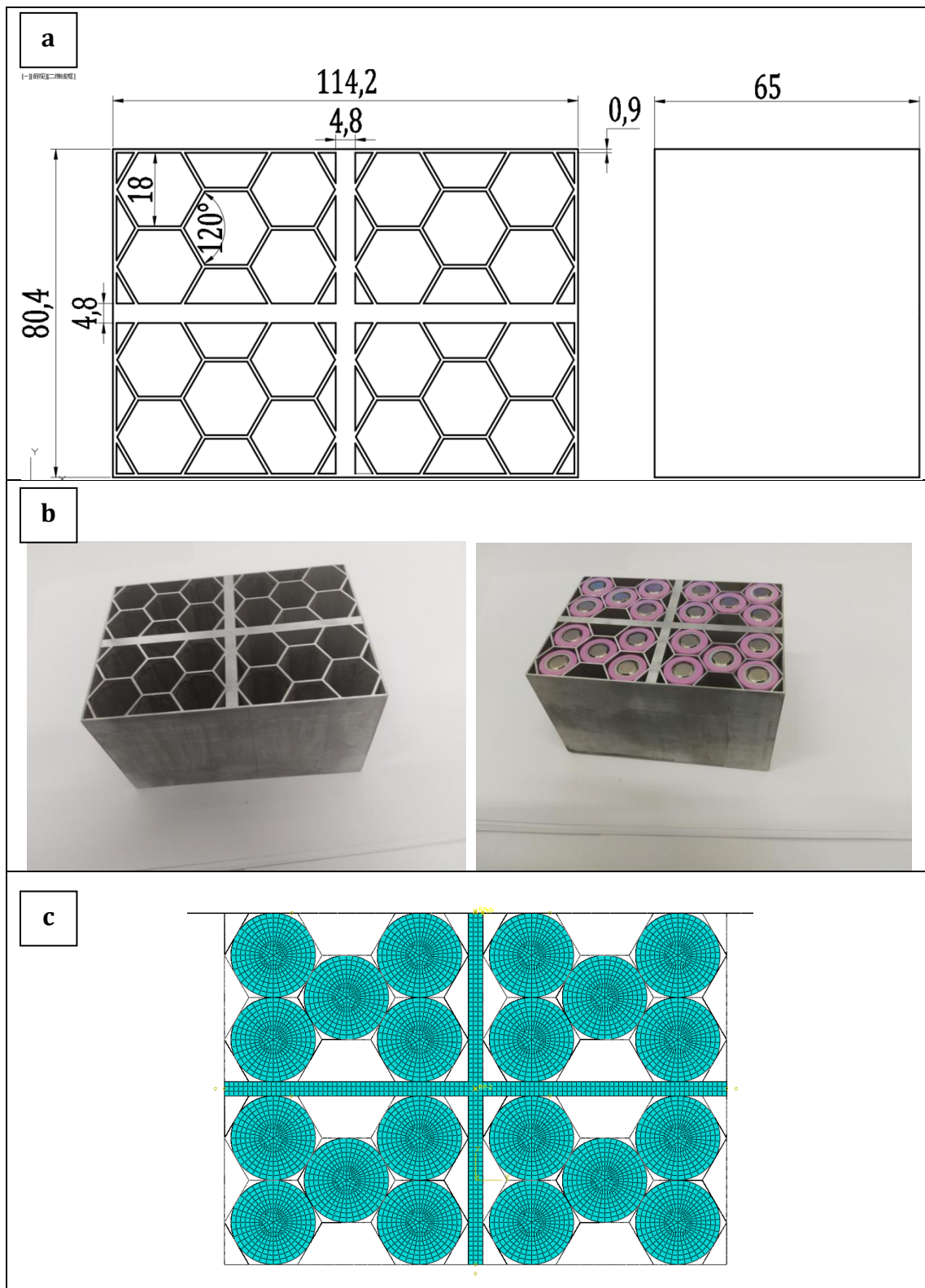
3.1 The validation of modeling method of battery package

3.1.1 Quasi-static compression test of battery package

In order to validate the modeling method of battery package, the quasi-static compression test was conducted to compare with FE model. The structure of the test battery package which without battery is shown in Fig. 5(a). Figure. 5(b) shows the test package sample. The quasi-static compression test was conducted

in INSTRON 2000kN Universal Test Machine. The compression rate is 1mm/min.

The deformed sample is shown in Fig. 5(d).



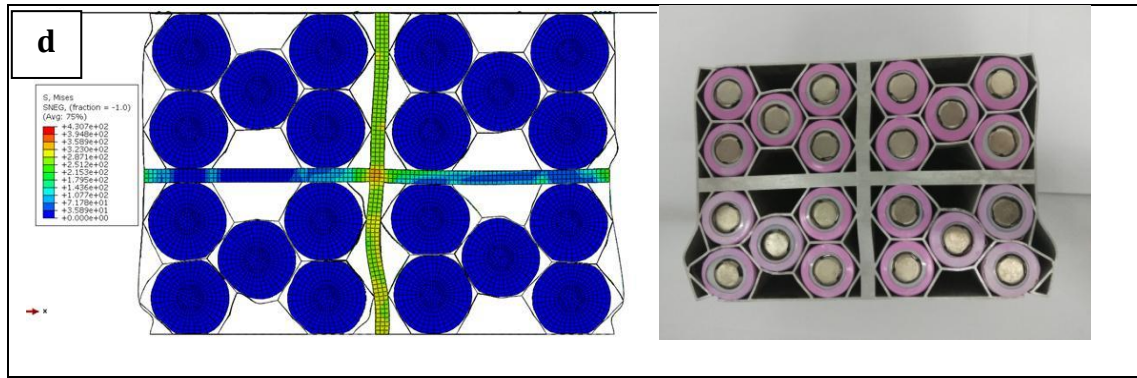


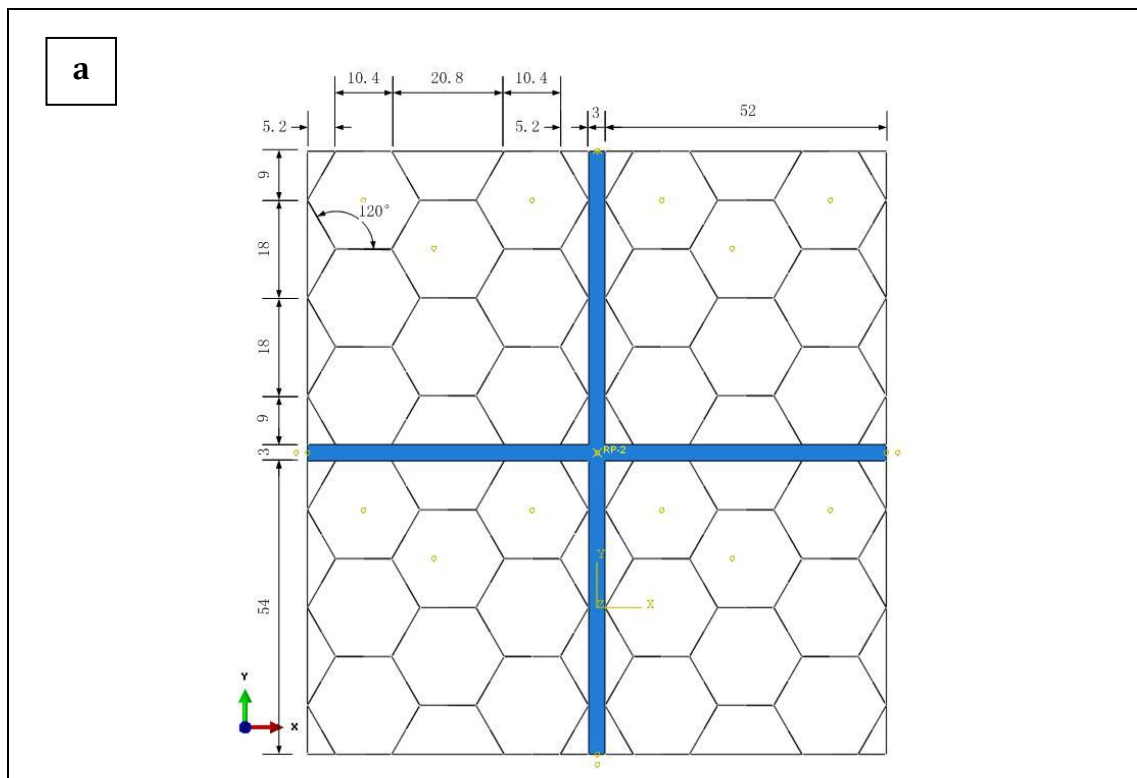
Fig. 5 (a) The structure of the battery package (b) The test package sample (c) The FE model of test sample (d) The stress contours of FE model and the deformed sample

3.1.2 The validation of modeling method

The material parameters of the whole package had been obtained. The FE model of battery package is constructed in ABAQUS. The FE model of the battery has been introduced in section 2. In order to improve the efficiency of simulation, the FE model is simplified and different from the entity. The thickness of honeycomb core is 0.9mm which is much less than the height of package 65mm. It could be modeled by shell element. Therefore, the FE model divided into two parts. One is the honeycomb core which is modeled by 4-nodes shell element (S4RSW). Another is the reinforce grid which is modeled by solid element (C3D8R). These two parts are tied together by using tie constraint. Figure. 5(c) shows the FE model of test sample. The displacement is 3mm. The stress contours of FE model is shown in Fig. 5(d). The deformed shape of test and simulation is similar by comparing the two pictures in Fig. 5(d).

3.2 Fine FE model of battery package

The structure of optimized battery package is shown in Fig. 6(a). The FE model of package also consisted of two parts which are honeycomb core and grid. The honeycomb core is modeled by using 4-node shell elements (S4RSW), its thickness is 0.9mm. The grid is modeled by using solid elements (C3D8R). Figure. 6(b) shows the FE model of the whole battery package. The simulation parameters are detailed in Table 6. Figure. 7(a) shows the stress contours of the package in 0s, 0.018s, 0.036s, 0.054s, 0.072s, respectively. These contours show the stress of model is increasing. In order to only show the integral stress contours of battery, the grid and honeycomb are excluded from the simulation output and only the battery are output as shown in Fig. 7(b). The maximum stress of battery was 32.1733MPa which is still in safe loading range.



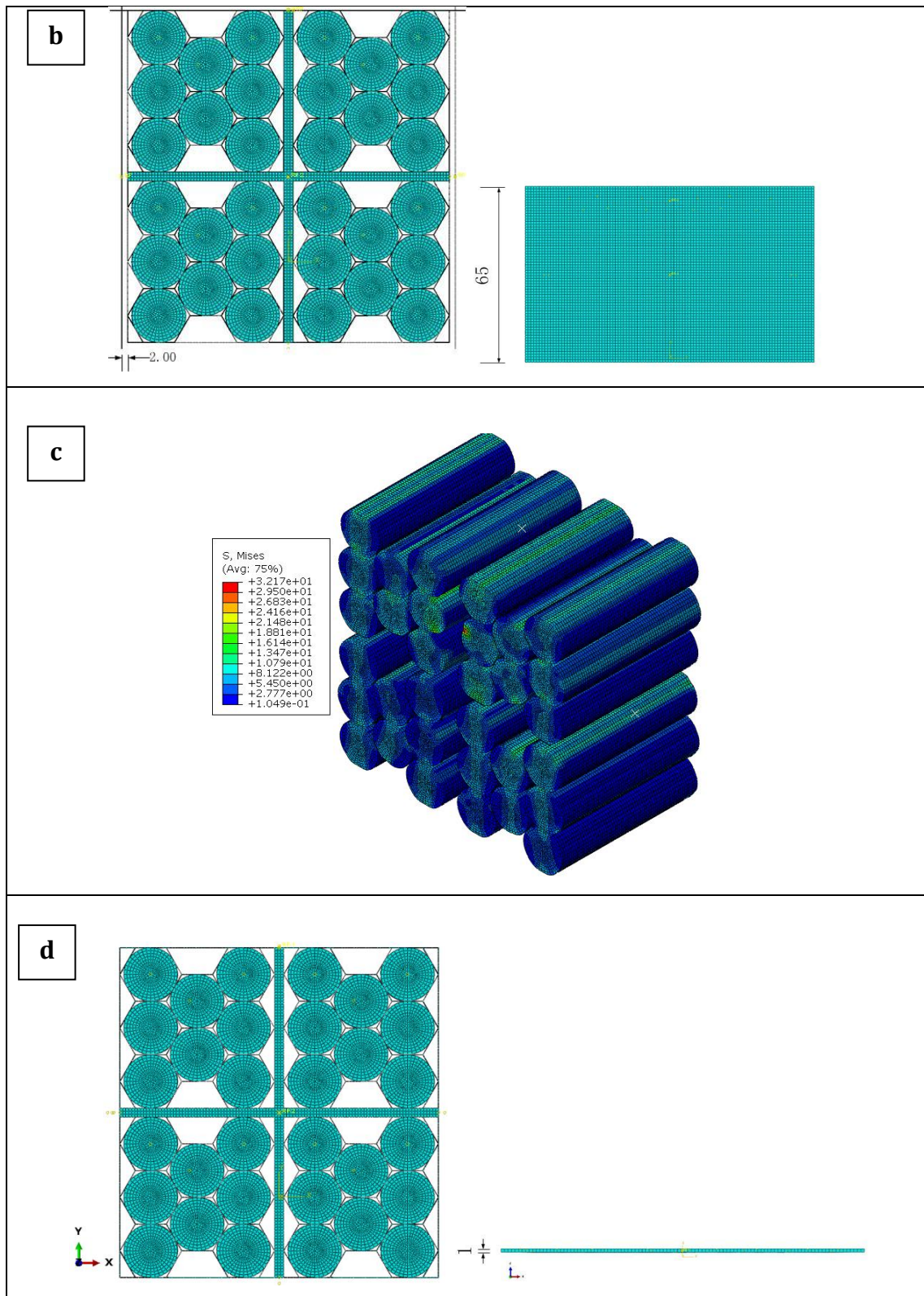
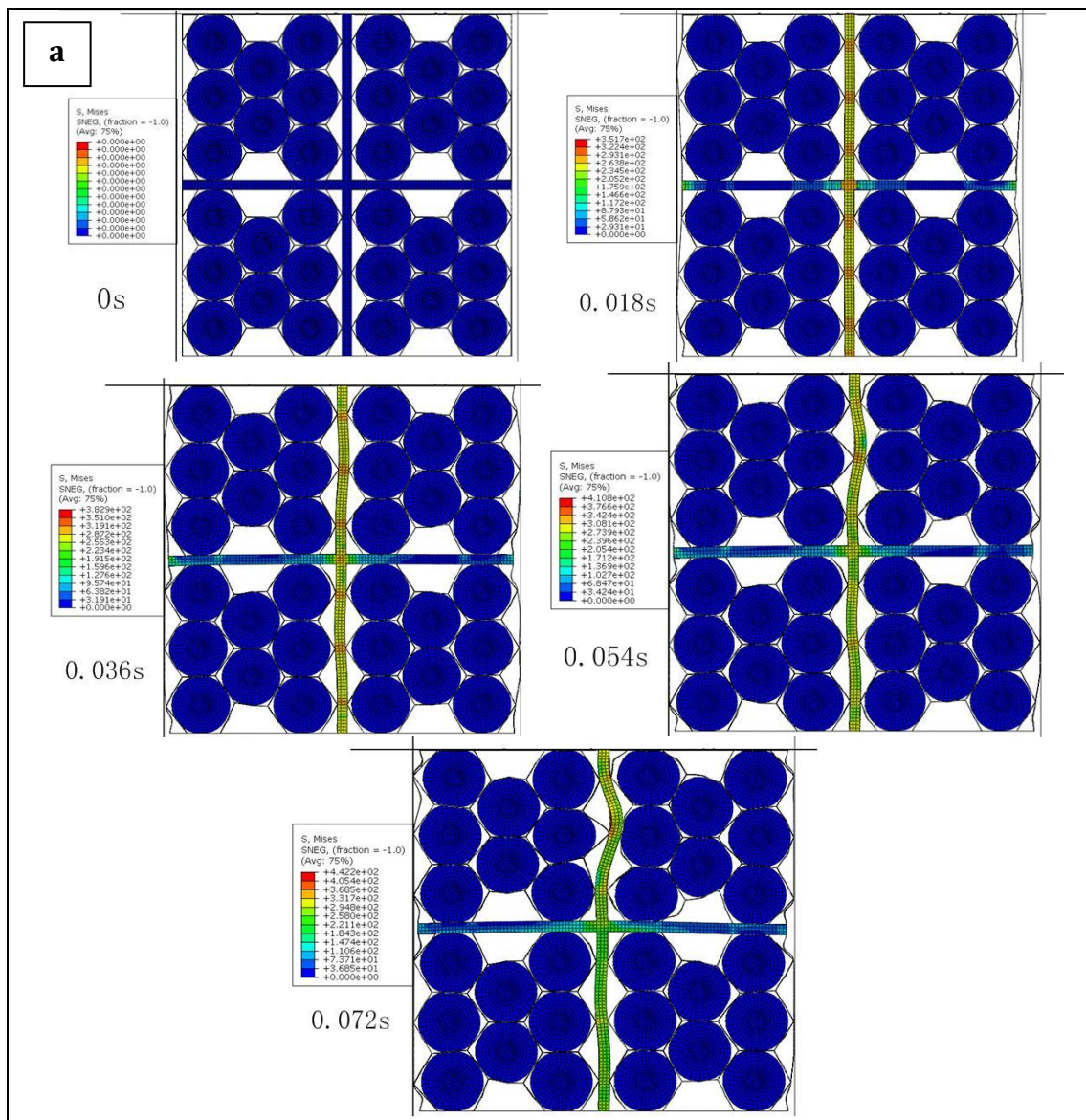


Fig. 6(a) The structure of optimized battery package(b) The FE model of the whole battery package (c) The stress contours of the batteries(d) The coarse FE model

Table 6

The simulation parameters of FE model of the battery package

Parameters	Values
Global seed size of the cell	1mm
Global seed size of the rigid shell	2mm
Global seed size of the grid	1mm
Global seed size of the honeycomb core	1mm
Simulation step	Dynamic explicit; 0.072s
Loading speed	80mm/s
Friction coefficient	0.17



b

Figure 10 displays the time evolution of the S -mises stress field. The figure is organized into four rows, each corresponding to a different time step: 0s, 0.018s, 0.036s, and 0.054s. Each row contains two plots of the stress field, showing the distribution of stress across a hexagonal lattice structure. The color scale for each plot indicates the magnitude of the S -mises stress, with values ranging from blue (low stress) to red (high stress). The stress field evolves over time, showing increasing stress levels and more localized stress concentrations within the lattice cells.

0s

0.018s

0.036s

0.054s

0.072s

c

0s

S, Mises
SNEG, (fraction = -1.0)
(Avg: 75%)

- +0.000e+00
- +0.000e+00
- +0.000e+00
- +0.000e+00
- +0.000e+00
- +0.000e+00
- +0.000e+00
- +0.000e+00
- +0.000e+00
- +0.000e+00
- +0.000e+00
- +0.000e+00
- +0.000e+00
- +0.000e+00
- +0.000e+00
- +0.000e+00
- +0.000e+00
- +0.000e+00

0.018s

S, Mises
SNEG, (fraction = -1.0)
(Avg: 75%)

- +3.697e+02
- +3.589e+02
- +3.081e+02
- +2.773e+02
- +2.465e+02
- +2.157e+02
- +1.849e+02
- +1.541e+02
- +1.232e+02
- +9.244e+01
- +6.162e+01
- +3.081e+01
- +0.000e+00

0.036s

S, Mises
SNEG, (fraction = -1.0)
(Avg: 75%)

- +4.124e+02
- +3.760e+02
- +3.436e+02
- +3.093e+02
- +2.749e+02
- +2.405e+02
- +2.062e+02
- +1.718e+02
- +1.375e+02
- +1.031e+02
- +6.873e+01
- +3.436e+01
- +0.000e+00

0.054s

S, Mises
SNEG, (fraction = -1.0)
(Avg: 75%)

- +4.131e+02
- +3.787e+02
- +3.443e+02
- +3.099e+02
- +2.754e+02
- +2.410e+02
- +2.066e+02
- +1.721e+02
- +1.377e+02
- +1.033e+02
- +6.886e+01
- +3.443e+01
- +0.000e+00

0.072s

S, Mises
SNEG, (fraction = -1.0)
(Avg: 75%)

- +4.527e+02
- +4.150e+02
- +3.773e+02
- +3.395e+02
- +3.019e+02
- +2.641e+02
- +2.264e+02
- +1.886e+02
- +1.509e+02
- +1.132e+02
- +7.545e+01
- +3.773e+01
- +0.000e+00

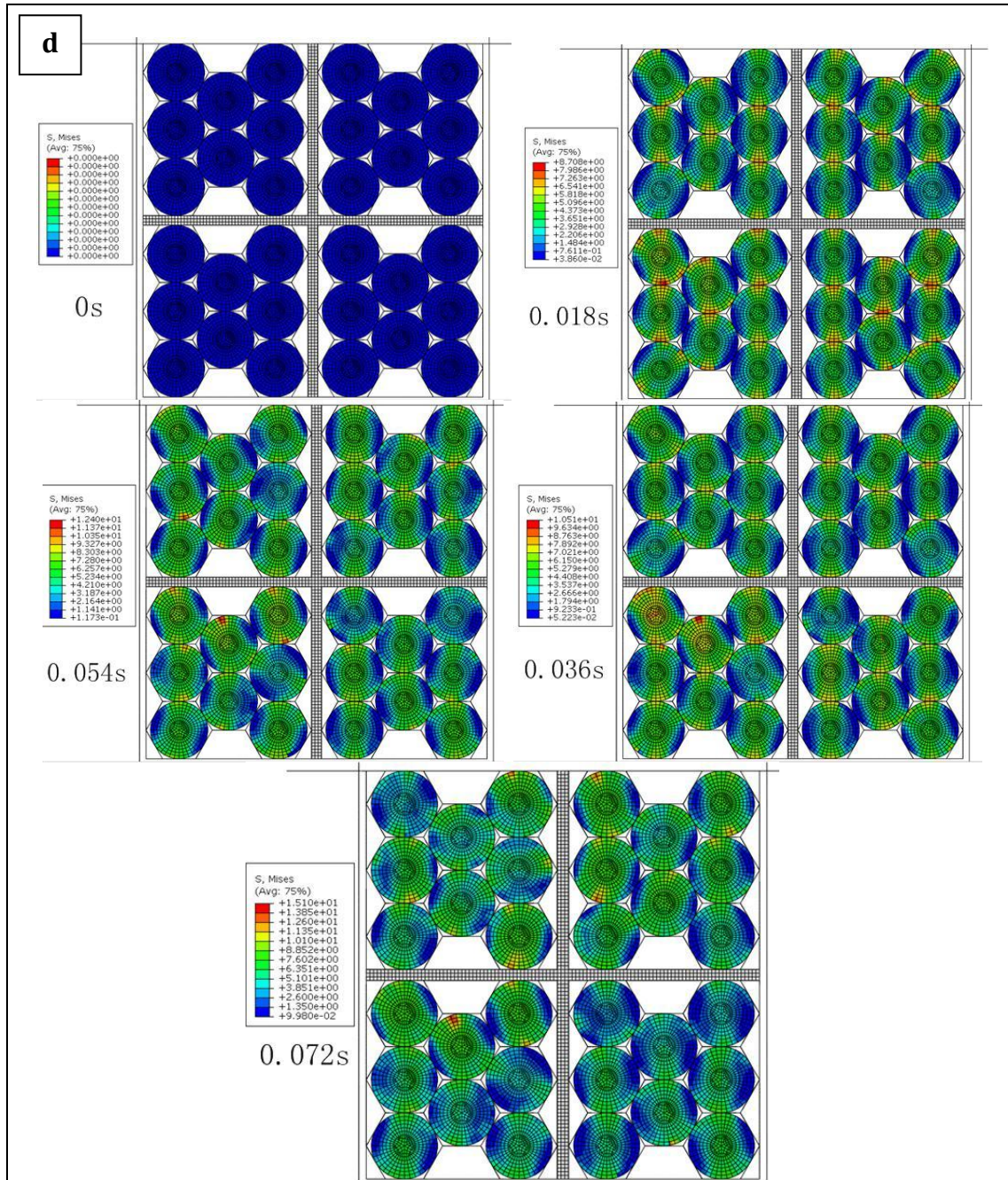


Fig. 7 (a) The stress contours of the fine FE model in different time (b) The stress contours of the battery of fine model in different time (c) The stress contours of coarse FE model (d) The stress contours of the battery of coarse model in different time

3.3 Coarse FE model of battery package

The fine FE model of battery package can simulate the stress-strain behaviors of the battery package accurately, however, the computational cost is high. It needs 2.5 hours to finish a simulation when use 8 CPUs. Therefore, the typical optimization method cannot be available for optimizing the battery package. However, SM algorithms are doing well in this kind of complex and expensive problems. Therefore, the SM algorithms be used in this study. In SM algorithms, an easier and cheaper FE model is needed which called coarse FE model. As shown in Fig. 6(c), the stress of battery was almost changeless in the axial direction of battery. Therefore, the fine FE model can be simplified as a pseudo-plane-strain model. The coarse FE model is shown in Fig. 6(d). All the nodes of battery and package were constrained their movement along the Z axis and their rotation along the X and Y axis. The simulation parameters of the coarse FE model were the same as the fine model. Figure. 7(c) shows the stress contours of coarse FE model in 0s, 0.018s, 0.036s, 0.054s, 0.072s, respectively. In order to show the integral stress contours of battery, the grid and honeycomb are excluded from the simulation output and only the battery are output as shown in Fig. 7(d). The maximum stress of battery is 15.1035MPa. The deformation of coarse FE model is similar with the deformation of fine FE model by comparing these two stress contours which in the same time. Because the coarse FE model needs only 5 minutes to finish a simulation and its stress states is similar to fine FE model, it can be an excellent coarse model of SM algorithms.

4. Optimization based on trust region space mapping (TRSM) method

4.1 Trust region space mapping

The TRSM might be the most widely used SM algorithm. Its characteristic is setting a trust region for design parameter of fine model. The trust region of every cycle is used to judge whether the algorithm is convergent. Then, the TRSM will be introduced in detail.

Assuming x is design parameter of fine model and f is the objective function of fine model. Similarly, the symbol z and c represents the design parameter and the objective function of coarse model, respectively. The optimization problem of fine model is expressed as

$$\min f(x) \quad (2)$$

The constraint function of fine model is $g_1(x)$ which is expressed as

$$g^l \leq g_1(x) \leq g^u \quad (3)$$

$$x^l \leq x \leq x^u \quad (4)$$

where g^l and g^u are the lower and upper bounds of constraint, respectively, x^l and x^u are the lower and upper bounds of design parameter x . The optimal solution of fine model is expressed as

$$x^* = \underset{x \in \Omega(f)}{\operatorname{argmin}} f(x) \quad (5)$$

The optimal solution of coarse model is expressed as

$$z^* = \underset{z \in \Omega^{(c)}}{\operatorname{argmin}} \quad c(z) \quad (6)$$

where $\Omega^{(f)}$ and $\Omega^{(c)}$ represent the design space of fine model and coarse model, respectively. The algorithms want to establish the mapping relation between the two design space, that is $p: \Omega^{(f)} \rightarrow \Omega^{(c)}$. The method to establish the relation is minimize the residual. The expression is

$$p(x) = \underset{z \in \Omega^{(c)}}{\operatorname{argmin}} \quad ||f(x) - c(z)|| \quad (7)$$

where $||f(x) - c(z)||$ is residual, and $|| \cdot ||$ is norm. According to the expression, it follows

$$f(x) \approx c(p(x)) \quad (8)$$

Therefore, the Equation. (4) can be transformed into

$$x^* \approx \underset{x \in \Omega^{(f)}}{\operatorname{argmin}} \quad c(p(x)) \quad (9)$$

Now, the complex and expensive optimization problem is transformed into easy and cheap problem. The specific algorithm steps are presented in Table 7. In every iteration, x_{k+1} is accepted if it satisfies

$$\zeta = \frac{c(z_k) - c(z_{k+1})}{c(z_k) - c(p_k(x_{k+1}))} \quad (10)$$

The update rule of B_k is

$$B_{k+1} = B_k + \frac{z_{k+1} - z_k - B_k h_k}{h_k^T h_k} h_k^T \quad (11)$$

where $h_k = x_{k+1} - x_k$.

The update rule of δ_k is

$$\delta_{k+1} = \begin{cases} 0.5 * \delta_k & \zeta \leq 0.01 \\ \delta_k & 0.01 \leq \zeta \leq 0.75 \\ \min(\delta_{max}, 2 * \delta_k) & \zeta \geq 0.75 \end{cases} \quad (12)$$

The algorithm converges if it satisfied any one of these conditions:

$$\begin{cases} k \geq k_{max} \\ ||h_k|| \leq \varepsilon_1(1 + ||x_k||) \\ \delta_k \leq \varepsilon_1(1 + ||x_k||) \\ \left| \frac{f(x_{k+1}) - f(x_k)}{f(x_k)} \right| < \varepsilon_2 \\ c(z_k) - c(p_k(x)) \leq 0 \end{cases} \quad (13)$$

where both ε_1 and ε_2 are constant coefficient, k_{max} is the maximum number of cycles

Table 7

TRSM algorithm

Given δ_0 ; set $B_0 = I(n, n)$, $k = 0$;

$z^* = \underset{z \in \Omega^{(c)}}{\operatorname{argmin}} c(z)$; $x_0 = z^*$;

Evaluate $f(x_0)$;

$z_0 = \underset{z}{\operatorname{argmin}} ||f(x_0) - c(z)||$;

While 1:

$x_{k+1} =$

$\underset{x \in \Omega^{(k)}}{\operatorname{argmin}} c(p_k(x))$, where $p_k(x) = B_k(x - x_k) + z_k$, $\Omega^{(k)} = \{x: ||x - x_k|| < \delta_k\}$;

Evaluate $f(x_{k+1})$;

$z_{k+1} = \underset{z}{\operatorname{argmin}} ||f(x_{k+1}) - c(z)||$;

Update B_k and δ_k ;

$k = k + 1$;

If algorithm converges:

Break;

End;

End;

4.2 optimization of battery package

In the optimization problem, the design variables are the lengthways thickness of grid h_1 , crosswise thickness of grid h_2 and thickness of honeycomb core h_3 . The range of these design variables are listed in Table. 8. Because the stress of battery is increasing with time, the stress state of battery in the final time is concerned. In order to improve the magnitude and distribution of stress of batteries, the optimized target is suggested to minimize the mean and variance of stress of all the batteries which in the final time. It is a multi-objective problem. The objective function is

$$\begin{cases} \min_{h_1, h_2, h_3} \text{mean}(\sigma) \\ \min_{h_1, h_2, h_3} \sigma^2(\sigma) \end{cases} \quad (14)$$

where σ is the stress of all batteries in 0.072s. GA was used to be the optimization algorithm of coarse model. The number of iteration is 20, and the size of population is 10. The initial population was selected randomly. The crossover percentage and the mutation percentage is 0.5, when the mutation rate is 0.02. Ultimately, GA obtained a series of feasible solutions, and the solution with minimum square sum of mean and variance was selected be the optimum solution. Then, the optimum solution obtained from coarse model was used to build the mapping relation with fine model and obtain the optimum solution of fine model.

The optimum solution of fine model is listed in Table 9. The initial mean and initial variance of stress of batteries in 0.072s was 5.3231MPa and 5.9944, respectively. The optimized mean and optimized variance of stress was

3.5836MPa and 4.3904, respectively. Figure. 8 shows the stress contours of the optimized fine model in 0s, 0.018s, 0.036s, 0.054s, 0.072s, respectively. The stress contours only output the stress of battery. The maximum stress of batteries was 12.9642MPa in 0.072s. It dropped by 59.71% compared to maximum stress of initial which is 32.1733MPa. The optimization consequence revealed the magnitude and distribution of stress of batteries has been improved significantly.

Table 8

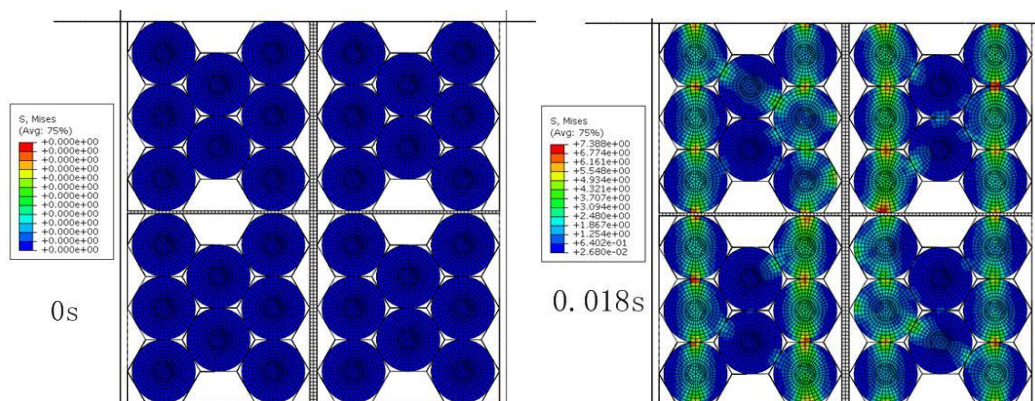
The range of design variables

Parameters/mm	Range
The lengthways thickness of grid h_1	[0.5,5]
The crosswise thickness of grid h_2	[0.5,5]
The thickness of honeycomb core h_3	[0.02,1]

Table 9

The optimum solution of fine model

Parameters/mm	Values
The lengthways thickness of grid h_1	2.0184
The crosswise thickness of grid h_2	0.8023
The thickness of honeycomb core h_3	0.03865



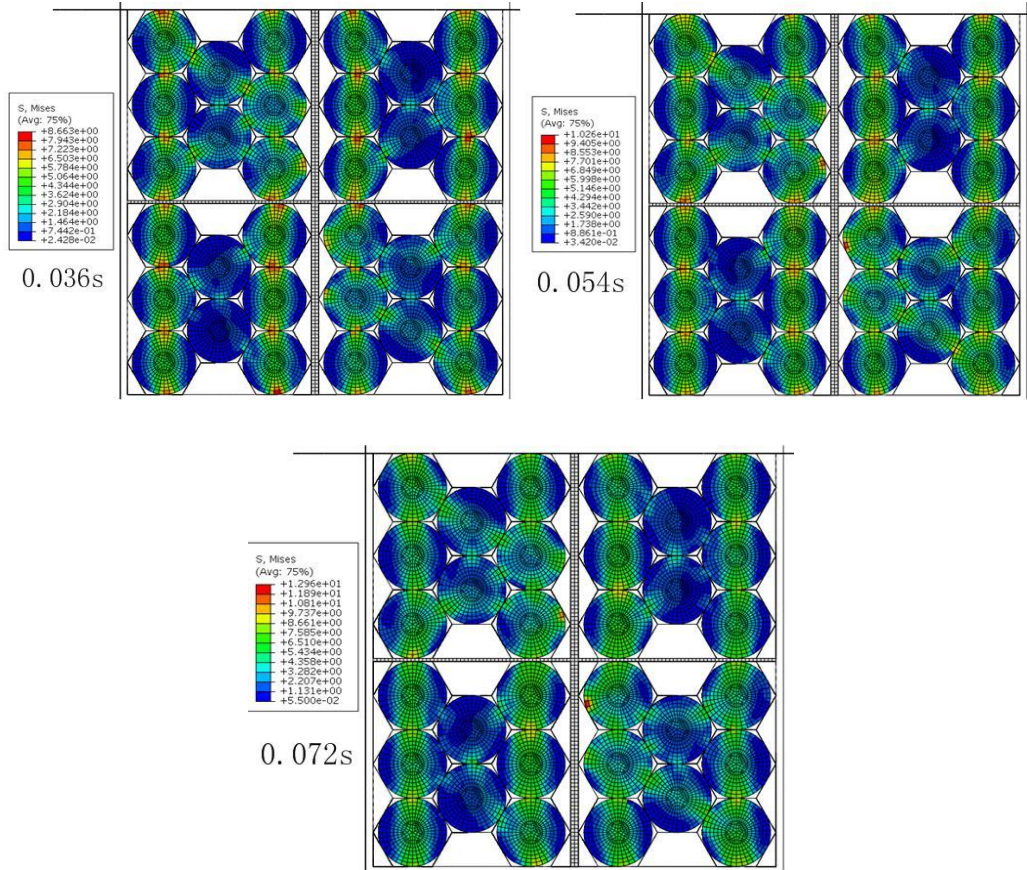


Fig. 8 The stress contours of the optimized fine model

5. Conclusions

A new honeycomb battery package structure is designed in this study. It is different from traditional honeycomb structure but using a grid to reinforce its strength. In order to develop the FE model of the package, the material parameters of battery and Al alloy have to be obtained. Therefore, the flat compression test of 18650 battery and the uniaxial tensile test of Al alloy 6061-T6 were conducted. And then according to the data that obtained from flat compression test of battery, the material parameters of battery were identified by inverse identification method. In order to validate the modeling method of battery package, the quasi-static compression test of battery package was conducted. The verification results revealed that the deformation shape of the

test package sample and the deformation shape of FE model is similar. Therefore, the FE model of battery package is accurate. In order to obtain the optimized structure of package, TRSM algorithm was used to optimize the structure. Compared with other SM algorithms, the coarse model of SM is based on a pseudo-plane-strain model. Moreover, to guarantee the reliability, the mean and variance values of battery stress are used to be the objective function. Optimized consequence shows the maximum stress of inner battery was decreased from 32.1733MPa to 12.9642MPa, the mean of battery was decreased from 5.3231MPa to 3.5836MPa and the variance was decreased from 5.9944 to 4.3904. The optimization effect is quite remarkable. Generally, the highlights of this work can be summarized as follows:

- A new structure of battery package is designed. It is a kind of honeycomb structure. In order to reinforce its strength, an Al alloy grid is used to be the framework.
- The material parameters of cylindrical battery are obtained by inverse identification method instead of replacing by material parameters of pouch battery.
- The TRSM algorithm is used to optimize the structure of battery package. Due to the expensive cost of FE evaluation, the typical optimization method cannot be available for optimizing the battery package. Therefore, the TRSM algorithm can be used to optimize the structure and obtain an ideal result in an acceptable time.

6. Acknowledgments

This work has been supported by National Key R&D Program of China

2017YFB0203701, Project of the Key Program of National Natural Science

Foundation of China under the Grant Numbers 11572120

References

- [1] Sun Z, Shi S, Guo X, et al. On compressive properties of composite sandwich structures with grid reinforced honeycomb core. *Composites Part B Engineering*, 2016, 94:245-252.
- [2] Meier J D. Material characterization of high-voltage lithium-ion battery models for crashworthiness analysis. 2013.
- [3] Sahraei E, Hill R, Wierzbicki T. Calibration and finite element simulation of pouch lithium-ion batteries for mechanical integrity. *Journal of Power Sources*, 2012, 201(3):307-321.
- [4] Greve L, Fehrenbach C. Mechanical testing and macro-mechanical finite element simulation of the deformation, fracture, and short circuit initiation of cylindrical Lithium ion battery cells. *Journal of Power Sources*, 2012, 214(4):377-385.
- [5] Sahraei E, Campbell J, Wierzbicki T. Modeling and short circuit detection of 18650 Li-ion cells under mechanical abuse conditions. *Journal of Power Sources*, 2012, 220(4):360-372.
- [6] Ali M Y, Lai W J, Pan J. Computational models for simulations of lithium-ion battery cells under constrained compression tests. *Journal of Power Sources*, 2013, 242(22):325-340.
- [7] Wierzbicki T, Sahraei E. Homogenized mechanical properties for the jellyroll of cylindrical Lithium-ion cells. *Journal of Power Sources*, 2013, 241(6):467-476.
- [8] Sahraei E, Meier J, Wierzbicki T. Characterizing and modeling mechanical properties and onset of short circuit for three types of lithium-ion pouch cells. *Journal of Power Sources*, 2014, 247(2):503-516.
- [9] Sahraei E, Bosco E, Dixon B, et al. Microscale failure mechanisms leading to internal short circuit in Li-ion batteries under complex loading scenarios. *Journal of Power Sources*, 2016, 319:56-65.

- [10] Yamashita M, Gotoh M. Impact behavior of honeycomb structures with various cell specifications—numerical simulation and experiment. *International Journal of Impact Engineering*, 2005, 32(1–4):618-630.
- [11] Ivañez I, Fernandez-Cañadas L M, Sanchez-Saez S. Compressive deformation and energy-absorption capability of aluminium honeycomb core. *Composite Structures*, 2017.
- [12] Zhang D, Fei Q, Zhang P. Drop-weight impact behavior of honeycomb sandwich panels under a spherical impactor. *Composite Structures*, 2017.
- [13] Leary S J, Bhaskar A, Keane A J. A Constraint Mapping Approach to the Structural Optimization of an Expensive Model using Surrogates. *Optimization and Engineering*, 2001, 2(4):385-398.
- [14] Redhe M, Nilsson L. Using Space Mapping and Surrogate Models to Optimize Vehicle Crashworthiness Design. 2013.
- [15] Florentie L, Blom D S, Scholcz T P, et al. Analysis of space mapping algorithms for application to partitioned fluid–structure interaction problems. *International Journal for Numerical Methods in Engineering*, 2016, 105(2):138-160.
- [16] Wang H, Fan T, Li G. Reanalysis-based space mapping method, an alternative optimization way for expensive simulation-based problems. *Structural & Multidisciplinary Optimization*, 2017, 55(6):2143-2157.